# Uneven Oxidation and Surface Reconstructions on Stepped Cu(100) and Cu(110)

Meng Li<sup>1</sup>, Matthew T. Curnan<sup>1,2†</sup>, Wissam A. Saidi<sup>2\*</sup>, Judith C. Yang<sup>1,3\*</sup>

<sup>1</sup>Department of Chemical and Petroleum Engineering, University of Pittsburgh, Pittsburgh, PA
15261, USA

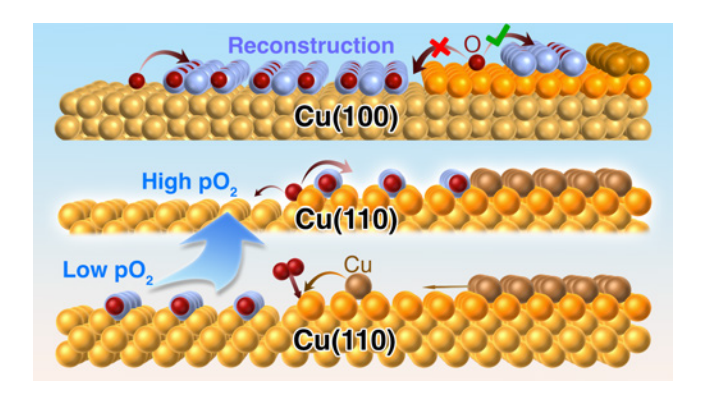
<sup>2</sup>Department of Mechanical Engineering & Materials Science, University of Pittsburgh,
Pittsburgh, PA 15261, USA

<sup>3</sup>Department of Physics and Astronomy, University of Pittsburgh, Pittsburgh, PA 15261, USA

KEYWORDS. Metal oxidation, surface reconstruction, surface step, Environmental TEM, *in situ* TEM, preferred oxidation

#### **ABSTRACT**

Surface step defects significantly impact gas-solid reactions and crystal growth. How defects such as surface steps affect oxidation, especially initial oxidation, is critical for nano-oxide applications in catalysis, electronics, and corrosion. We posit that surface reconstruction, a crucial intermediate oxidation step, can highlight initial oxide formation preferences and thus enable bridging the temporal and spatial scale gaps between atomistic simulations and experiments. We investigate the surface-step induced uneven surface oxidation on Cu(100) and Cu(110), using atomic-scale *in situ* Environmental Transmission Electron Microscopy experiments with dynamical gas control and advanced data processing. We show that Cu(100)-O missing row reconstruction strongly favors upper terraces over lower terraces while Cu(110)-O (2×1) "added row" reconstructions indicate slight preferences for upper or lower terraces, depending on oxygen concentration. The observed formation site preference and its variation with surface orientation and oxygen concentration are mechanistically explained by Ehrlich–Schwöbel barrier differences for oxygen diffusion on stepped surfaces.



Surface steps are commonly observed, significant defects on realistic surfaces. Given the atoms comprising step edges are undercoordinated, surface steps are considered active sites for heterogeneous catalysts due to their enhanced binding with reactant molecules<sup>1-4</sup>, improved bond-breaking activity<sup>2, 5</sup>, capabilities to stabilize single atom catalysts<sup>6,7</sup> and change the stability of catalytically active phase<sup>8</sup>. Besides catalytic applications, surface steps are also important sites for crystal growth and erosion<sup>9</sup>, serving as sources and sinks for diffusing atoms and controlling atomic diffusion<sup>10</sup>. Surface oxidation is a process that involves initial dissociative O absorption, metal surface reconstruction due to interactions with a gaseous environment, and subsequent oxide nucleation and growth<sup>11, 12</sup>. How surface steps affect this oxidation process, especially its initial stages, is critical for fundamental understanding of oxidation, and advanced design and manufacturing of nano-oxide for applications in catalysis, electronics, and quantum computing<sup>13-16</sup>

Classical oxidation theories only describe the oxidation of flat surfaces, while the effect of surface steps or other defects on oxidation is still not clear. Surface steps have been found to affect oxygen absorption and mass diffusion in theoretical simulations<sup>17-20</sup>, and enhance observed oxide growth rates in experiments<sup>21, 22</sup>. However, early-stage computational models of oxygen adsorption and diffusion are separated from experimental observations of late-stage oxide growth by large temporal and spatial gaps. Surface reconstruction, or the structural transformation of metal surfaces under oxygen, is a key intermediate step occurring between early-stage oxygen adsorption and late-stage oxide growth processes observed in many metals and alloys<sup>11, 23-25</sup>. Limited by computational cost, existing simulation methodologies, such as Density Functional Theory (DFT) and Molecular Dynamics (MD), cannot fully model the oxidation processes associated with surface reconstruction. Instead, such simulations can predict possible O accumulation sites on

clean stepped surfaces, as such sites indicate where surface reconstructions can form. Limited by the time and spatial resolution of current experimental methods, direct experimental observation of surface O accumulation sites on clean surfaces is an extremely challenging task. Instead, experimental observation of incipient surface reconstruction can trace where O accumulates. Hence, by evaluating surface reconstruction formation processes on stepped surfaces, experiment and simulation can be more comprehensively bridged, elucidating how surface steps affect oxidation.

With respect to experimental methodology, Scanning Tunneling Microscopy (STM) is widely used to identify static surface reconstruction structures. However, the dynamic processes reconstructing stepped surfaces are still unclear due to the lack of temporal resolution. *In situ* Environmental Transmission Electron Microscopy (ETEM) is an emerging new technique to study the atomic processes of gas-solid reactions. ETEM has shown great potential towards revealing the atomic processes underlying oxide growth<sup>26</sup>, reduction<sup>27</sup>, and even some reconstruction phases<sup>25</sup>. However, capturing comprehensive reconstruction formation dynamics is very challenging, given sample drift caused by gas injection<sup>28</sup> coincides with the fast dynamics of surface reconstruction formation. Also, the lack of ultra-high vacuum capability in current ETEMs prevents precise gas control within the low-pressure ranges that characterize surface reconstruction reactions.

In this work, we investigated the dynamic formation of surface reconstructions on stepped Cu(100) and Cu(110) surfaces using atomic resolution *in situ* ETEM and advanced data analysis. Through our methodology, meticulously controlled low-pressure O<sub>2</sub> was introduced to clean Cu surfaces at elevated temperatures to slow down surface reconstruction formation dynamics. Further, a Python package was developed to mitigate the drift in High-Resolution TEM (HRTEM)

movies, so that the entire process of surface reconstruction formation proceeding from gas injection could be recorded at the atomic scale. Cu(100)- $(2\sqrt{2} \times \sqrt{2})R45^{\circ}$ -O missing row reconstructions (referred to as MRR for short hereafter) are found to prefer formation on upper Cu(100) terraces. Cu(110)- $(2\times1)$ -O added row reconstructions (referred as  $(2\times1)$  for short hereafter) slightly prefer formation on lower terrace sites near step edges under low oxygen concentration, while they slightly prefer upper terrace formation under higher oxygen concentrations. These results are consistent with our previous theoretical predictions made using DFT and  $MD^{17-19}$ . The mechanisms for the reconstruction formation processes on stepped Cu(100) and Cu(110) surfaces are explained. By narrowing the gap between experimental and theoretical resolution of surface step oxidation, these results enhance the current understanding of surface oxidation processes. Furthermore, this work provides a powerful and promising method to study the dynamics of the inchoate stages of surface oxidation, which can be generalized to additional compositions, interfacial defect structures, and reaction processes.

## **Materials & Methods**

Single crystalline Cu(001) thin films with faceted holes were used to observe surface reconstruction dynamics under ETEM. Cu(001) thin films are prepared using Ultra-High-Vacuum *e*-beam evaporation (Pascal Technologies UHV Dual *e*-beam Evaporator) on NaCl(100) substrates, and are then transferred to TEM grids using the float-off method introduced in our previous work. In situ ETEM observation was performed using the Hitachi H-9500 ETEM with a Hitachi double-tilt heating holder and a homemade gas delivery system with three gas injection lines. The gas injection lines are connected to the pumping system of the ETEM, so that residual gas in the pipeline can be quickly removed and gas changes can be finished within minutes. To facilitate the surface reconstruction experiments at low gas pressure, the gas chamber was baked

before each experiment to remove residual gases and contaminations. Cu thin films are reduced under 1 Pa H<sub>2</sub> at 600 °C to remove oxides, as well as to create faceted holes. These faceted holes consist of Cu(100) and Cu(110) facets, enabling observation of surface reconstruction dynamics from a cross-sectional view and creating many surface steps on which their effects can be investigated. After forming these faceted holes, samples were cooled to 300 °C under flowing H<sub>2</sub> until thermal drift diminished sufficiently to allow HRTEM observation. After thermal drift attenuated, the H<sub>2</sub> gas source was cut off, then the gas line and the specimen chamber were pumped down to vacuum (~3×10<sup>-5</sup> Pa). Afterward, O<sub>2</sub> gas was gradually injected through another gas line. To capture the dynamic process of surface reconstruction formation, precisely controlled low O<sub>2</sub> partial pressures between 2.5×10<sup>-4</sup> and 1.0×10<sup>-2</sup> Pa were gradually injected. *In situ* HRTEM observation was carried out on the Cu(100) and Cu(110) facets during gas injection at 300 °C. Real-time movies were recorded using a Gatan Orius 833 CCD camera with a frame rate of 5 frames/s. To avoid electron beam effects on the observed results, low-dose imaging condition was applied in our investigations (e-beam dosage:  $\sim 138 \text{ nA/um}^2 \text{ or } 8.6 \times 10^5 \text{ e/nm}^2 \cdot \text{s}$ ), which is lower than that normally used for HRTEM imaging  $(\sim 1-5 \times 10^6 \text{ e/nm}^2 \cdot \text{s})^{29}$ . The reconstruction phases are stable under the e-beam, and reconstructions are observed on areas with and without e-beam under the same O<sub>2</sub> pressure, indicating the e-beam effects on the surface reconstruction experiment are not significant.

As-recorded movies contain significant drift due to gas injection<sup>28</sup>. To focus on atomic-scale reconstruction formation processes, movies need to be aligned frame-by-frame at the atomic level. However, dedicated tools for aligning *in situ* HRTEM movies are lacking. Existing methods for alignment require using unchanging features as tracking markers, which work poorly on *in situ* TEM movies with fast-changing features and low signal-to-noise ratio. Besides, image blur due to

sample drift and focus change also significantly deteriorate alignment results. To solve these problems, we developed a Python package for *in situ* HRTEM movie processing. This package automatically detects blurry frames and removes them during the alignment process, while an improved adaptive template matching algorithm aligns remaining frames to produce *in situ* (HR)TEM movies. With the help of this package, atomic-scale surface reaction dynamics during gas injection can be fully studied, facilitating a broader understanding of surface reaction dynamics at the atomic level.

#### **Results & Discussion**

### **Experimentally Observed Surface Reconstruction**

Figure 1 shows HRTEM images of Cu(100) and (110) surfaces in vacuum and under  $O_2$ . For Cu(100) surfaces, surface layers share the same structures as bulk layers in vacuum, indicating unreconstructed surfaces (Figure 1a). As depicted in Figure 1b, surface layer lattice spacing increased from 1.8 Å to 2.1 Å under  $O_2$ , while surface atoms formed patterns comprised of single column missing rows from every fourth atom, which matches the structure of the Cu(100)- $(2\sqrt{2} \times \sqrt{2})R45^{\circ}$  -O missing row reconstruction (MRR, Figure 1c) from literature<sup>30-33</sup>, as confirmed by HRTEM image simulation (Figure 1b, inset). In the MRR structure, O combine with Cu to form Cu-O chains along the (001) direction, ejecting one Cu row per four atomic rows. For Cu(110) under low  $O_2$  pressure, surface layers changed from pristine (1×1) (Figure 1d) to (2×1) sawtooth "added row" structures (Figure 1e), as confirmed by HRTEM image simulations (Figure 1e, inset). Figure 1f shows the corresponding atomic structure of the Cu(110)-(2×1)-O reconstruction, with one Cu-O chain added per two Cu atomic rows. Under higher  $O_2$  pressure, Cu(110)-c(6×2)-O reconstruction phases are observed to form on (2×1) reconstructed surfaces

(Figure 1g-h). These structures are consistent with previous experimental (STM) and theoretical predictions<sup>34-36</sup>.

# Formation of MRR on Stepped Cu(100) Surface

After confirming the MRR structure, in situ ETEM experiments on stepped Cu(100) surfaces are performed. Movie S1 and Figure 2 show typical MRR formation processes on stepped Cu(100) surfaces. Initially, the surfaces were unreconstructed in vacuum (blue colored) with two monolayer-height surface steps (labeled 1-2) on the right side of the sample (Figure 2a). When 7×10<sup>-3</sup> Pa O<sub>2</sub> was injected, Figure 2b shows the step location (1-2) remained unchanged, while a new monolayer-height step (labeled 3) developed from the leftward sample side. Upper terrace areas near steps 1-3 showed clear lattice spacing increases and new MRR formation (red-colored regions), indicating these areas were the first to develop MRR phases. Later, another new surface step (labeled 4, Figure 2c) formed on the leftward sample side, while MRR nucleated on its upper terrace. Meanwhile, step 2 expanded while step 1 shrunk, indicating Cu mass transport between these different layers. Following MRR nucleation on upper terraces, MRR structures originated on lower terrace step sites (Figure 2d). Afterward, MRR phases expanded from upper and lower terrace sites until the entire sample surface was covered (Figure 2e). Similar results depicting preferred MRR formation on upper terraces are observed at 350, 400, 450, and 500 °C, as shown in Movie S2.

## Formation of (2×1) Reconstruction on Stepped Cu(110) Surface

Similar experiments on reconstruction formation are performed on stepped Cu(110) surfaces. Compared with Cu(100), Cu(110) (2×1) reconstructions start to develop at much lower O<sub>2</sub> pressures, consistent with literature stating that O<sub>2</sub> dissociation on Cu(110) is an order of

magnitude faster than on  $Cu(100)^{37,38}$ . Under  $7.8\times10^{-3}$  Pa  $O_2$ , Cu(110) surfaces changed to  $(2\times1)$  phases within a second (Figure 3d and Movie S6) and then gradually transformed to  $c(6\times2)$  reconstructions, indicating evaluated  $O_2$  pressures are well beyond the O coverage threshold required for  $(2\times1)$  reconstruction formation. To capture dynamic reconstruction formation processes on Cu(110), lower  $O_2$  pressures from  $2.3\times10^{-4}$  Pa to  $7.8\times10^{-3}$  Pa were tested. Among these tests,  $2.3\times10^{-4}$  Pa is the minimum gas pressure for the injected gas in our instrument. The  $c(6\times2)$  reconstruction formed on  $(2\times1)$  reconstructed surfaces under pressures above  $\sim3.4\times10^{-3}$  Pa. Probing oxidation processes that occur during the  $(2\times1)$  to  $c(6\times2)$  phase transformation on stepped Cu(110) surfaces is beyond current simulation capability, thus we only focus on pertinent  $(2\times1)$  formation at pressures from  $2.3\times10^{-4}$  Pa to  $7.8\times10^{-4}$  Pa.

As shown in Figure 3a and Movie S3, under low O<sub>2</sub> concentrations (2.3×10<sup>-4</sup> Pa), (2×1) phases slightly prefer developing on lower terraces. Initially, two monoatomic-height grooves separated steps 1&2 and 3&4. At 43.8 s, (2×1) added row phases (colored red) formed on lower terraces (steps 2, 4, and 5). (2×1) phases were located adjacent to surface steps, indicating new (2×1) phases grow from near step edges to lower terraces. At 50.2 s, (2×1) phases form on upper terraces (steps 1&4), then expand on lower and upper terraces while retreating from their steps of origin (steps 2&3), indicating that Cu detach from surface steps to form added Cu-O rows.

Under higher  $O_2$  concentration (7.8 ×10<sup>-4</sup> Pa), as shown in Figure 3b and Movie S4, (2×1) formation slightly prefers upper terraces. Initially, a monoatomic-height groove separates steps 2&3 and step 1 (Figure 3b). At 28.6 s, (2×1) phases form on the upper terrace (step 2) next to step edges, inferring step edges source Cu-O chain growth. Further  $O_2$  injection depicts more (2×1) domain formation on the upper terraces of each step, until (2×1) phases cover entire sample surfaces. This phenomenon remains consistent under even higher  $O_2$  pressures, as shown in Figure

3d and Movie S6. In comparison, under medium  $O_2$  concentration (4.7 ×10<sup>-4</sup> Pa), as shown in Figure 3c and Movie S5, (2×1) formation initiates at both upper and lower terraces near the step edge and then expands to the entire surface. Previous STM experiments showed contradicting location preferences on upper or lower terraces for (2×1) formation<sup>39, 40</sup>, leaving the effect of steps on Cu(110) initial oxidation debatable. Our result indicates that this contradicting preference is caused by differences in  $O_2$  concentration, suggesting a competing mechanism for (2×1) formation.

## Effect of Surface Step on Cu(100) MRR Formation

As shown in Figure 1c, O combines with surface Cu on flat Cu(100) surfaces to form Cu-O chains, while surface Cu is ejected to form missing rows every fourth column.<sup>30, 41</sup> Previous DFT simulation on MRR formation suggests that Cu ejection is energetically favored by the presence of surface-absorbed  $O_2$  molecules, and the rate-limiting steps are  $O_2$  dissociation ( $E_a = 0.95 \text{ eV}$ ) and Cu ejection ( $E_a = 0.96 \ eV$ )<sup>41</sup>. Hence, surface Cu ejection and O distribution could affect reconstruction formation dynamics. Compared with flat Cu(100) surface, stepped surface promotes the dissociation of O<sub>2</sub>.<sup>38</sup> Moreover, our previous O diffusion simulations found unusual negative Ehrlich-Schwöbel (E-S) barriers, such that the energy barrier for ascending O diffusion converges to 0.30 eV lower than that of corresponding descending O diffusion for monolayerheight step<sup>19</sup>. This leads to preferred O ascending diffusion on stepped surfaces, which would likely ultimately produce O accumulation on upper terraces. Beyond O diffusion changes coinciding with unevenly distributed oxygen adatoms, Cu mass transport from step edges to flat terraces is also enhanced in MD simulations.<sup>17</sup> Therefore, as illustrated in Figure 4a-c, Cu(100) surface steps induce more O accumulation on upper terraces, which in turn promotes Cu ejection on upper terraces and leads to preferred MRR formation on them. Besides upper terraces, lower

terraces near step edges tend to experience more O accumulation than flat terraces, leading to the observed MRR formation order of upper terraces, then lower terraces near step edges, and finally flat terraces.

## Effect of Surface Step on Cu(110) (2×1) Reconstruction Formation

For Cu(110) surfaces, (2×1) reconstruction development requires Cu and O atoms to form Cu-O added rows<sup>42</sup>. With surface steps, Cu detached from surface steps, together with Cu diffused from surrounding facets, could source Cu for such rows. Cu diffusion over Cu(110) steps exhibits a positive E-S barrier of 0.12 eV<sup>43</sup>, favoring descending diffusion. Hence, more diffusing Cu detaches from step edges and diffuse on lower terraces near step edges.

Under low oxygen concentration (Figure 4d-f), the surface is lack of diffusing O, O<sub>2</sub> dissociation on Cu(110) surfaces sources O for Cu-O added rows. Compared with flat Cu(110) surfaces, step edge facets strongly favor dissociative O<sub>2</sub> adsorption.<sup>18, 32, 44</sup> Hence, O adatoms accumulate near step edges. Oxygen on the step edge leads to formation of Cu-O chain along the step edge. This Cu-O chain blocks the detachment of Cu from this step edge, while Cu diffused from nearby steps could serve as Cu source for further Cu-O chain formation parallel to the step edge. Meanwhile, in the presence of O atoms nearby, more Cu atoms detach from nearby step edges, diffusing on adjacent lower terraces. Hence, (2×1) reconstructions are observed to slightly prefer lower terraces near step edges under low oxygen concentration.

Under higher oxygen concentrations (Figure 4g-i), the surface is rich in diffusing O, O atoms diffusing on surfaces source O for Cu-O added rows. In contrast with large negative O diffusion E-S barriers on Cu(100) steps, previous DFT simulations suggest that O diffusion barriers for ascending and descending Cu(110) surface steps are comparable, as they are primarily determined

by the same structures impeding O diffusion along (100) step edge facets.<sup>18</sup> MD simulations infer slightly more O will cover Cu(110) step upper terraces than lower terraces, though this difference is small relative to O coverage differentials over other Cu orientations.<sup>18</sup> Thus, the amount of O on upper and lower terraces near step edges are greater than that on flat surfaces, and slightly more O on the upper terrace. Hence, (2×1) reconstructions develop on Cu(110) step upper and lower terraces, slightly preferring the former at higher oxygen concentrations.

#### **Conclusion**

In summary, we performed atomic resolution *in situ* ETEM experiments to study the effects of surface steps on the formation of surface reconstructions under oxygen at 300 °C. For stepped Cu(100) surfaces, MRRs first preferably form on upper terraces, followed by lower terraces near step edges, then flat terraces. This phenomenon can be explained by negative O diffusion E-S barriers on stepped Cu(100), which lead to more oxygen accumulation on upper terraces. For stepped Cu(110) surfaces, (2×1) reconstruction formation prefers step regions over flat surfaces, though preferred formation sites vary with O<sub>2</sub> concentration. Under low oxygen concentrations, (2×1) reconstructions slightly prefer lower terraces near their step edges, while such reconstructions slightly prefer upper terraces under higher oxygen pressures. This difference is due to the change of O source from absorbed oxygen at lower concentrations to diffusing O atoms at higher concentrations. Such differences in reconstruction preferences between Cu(100) and Cu(110) surfaces demonstrate how E-S barriers affect the oxidation process.

Besides kinetic factors such as Cu and O diffusion, thermodynamic factors such as nucleation barriers for reconstruction formation should also be considered. The formation of MRR on Cu(100), and  $(2\times1)$  reconstruction on Cu(110), both lead to decrease in surface energies<sup>32, 41, 42</sup>. The

energy barrier for MRR formation on Cu(100) (0.96 eV) is higher than that for (2×1) formation on Cu(110) (0.73 eV), which in addition to the difference on O<sub>2</sub> dissociation preference on Cu(110) over Cu(100), these barriers elucidate how (2×1) forms on Cu(110) much more quickly than MRR on Cu(100) under the same O<sub>2</sub> pressure. In terms of reconstruction formation for the same orientation with and without steps, the upper and lower terraces are equivalent in factors such as their defect density and orientation. Furthermore, correlations between O diffusion barrier ratios and oxide growth preferences across different stepped interfaces – coupled with how O diffusion barriers are large (0.66-1.34 eV) relative to corresponding surface reconstruction kinetic barriers and thermodynamic impediments – indicate that rate-limiting O diffusion would likely determine oxide growth preferences observed in this study.<sup>20</sup> Thus, we do not expect thermodynamic factors such as surface strain to differentiate studied stepped surfaces relative to oxide growth preferences.

Using oxygen-induced surface reconstruction as a tracer, our experimental results not only confirmed previous theoretical predictions for step-edge-directed metal oxidation, but also elucidated complete mechanisms for surface reconstruction formation on stepped surfaces. These findings can be generalized to additional metals, alloys, and even other defect structures. Further, the step-edge induced non-uniform gas distribution extends beyond gas-solid reactions applying O<sub>2</sub>, encompassing multiple gaseous reactants – such as H<sub>2</sub>, CO<sub>2</sub>, CO, and H<sub>2</sub>O – that can feature E-S barrier effects. Our work demonstrates that *in situ* ETEM with advanced data analysis can not only dynamically identify atomic-scale surface reactions at their immediate inception, but also powerfully and promisingly characterize such dynamics over entire reactions at high temporal and spatial resolution. Such accomplishments bolster applications including atomic-scale advanced electronics manufacturing, catalyst design, localized surface decoration, and corrosion-resistance design.

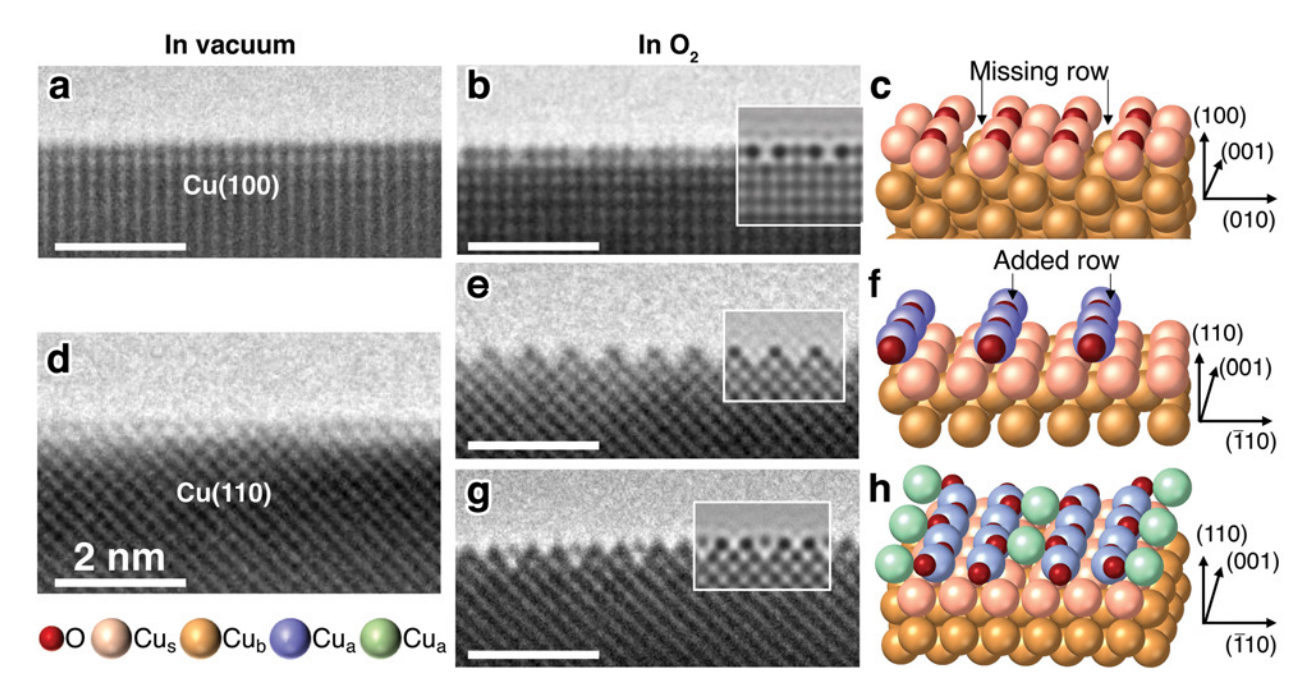


**Figure 1.** HRTEM images of surface reconstructions on Cu(100) and (110) surfaces. **(a-c)** Cu(100) surface layers changed from **(a)** unreconstructed in vacuum to **(b)** MRRs in  $O_2$ , with a corresponding simulated HRTEM image ((b), inset) made using the atomic structure of MRR shown in **(c)**. **(d-h)** Cu(110) surface layers changed from **(d)** unreconstructed (1×1) in vacuum to **(e)** (2×1) reconstructions under low  $O_2$  pressure ( $\sim 7 \times 10^{-4}$  Pa  $O_2$ ), with a simulated HRTEM image ((e), inset) made using the atomic structure shown in **(f)**. Under higher  $O_2$  pressure, a **(g)** Cu(110)-O c(6×2) reconstruction phase forms on the Cu(110) (2×1) reconstructed surface, with simulated HRTEM image ((g), inset) using the c(6×2) atomic structure shown in **(h)**. Atomic models highlight surface Cu (Cu<sub>s</sub>, pink), bulk Cu (Cu<sub>b</sub>, beige), O atoms (red), and added Cu forming (2×1) (Cu<sub>b</sub>, blue) and c(6×2) (Cu<sub>b</sub>, green) phases. Scale bars indicate 2 nm in all images.

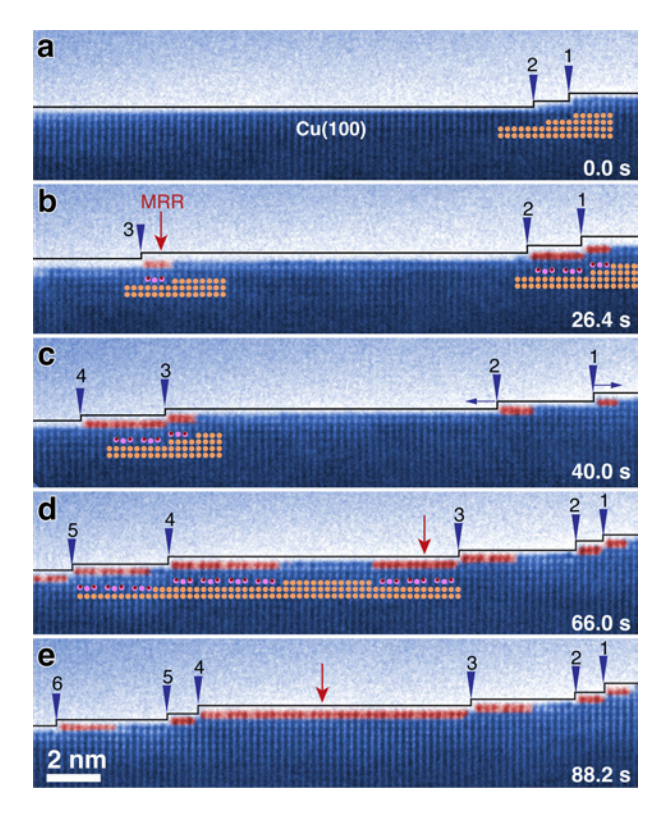


**Figure 2.** Formation of MRR on stepped Cu(100) under 7×10<sup>-3</sup> Pa O<sub>2</sub> at 300 °C. (a) Before O<sub>2</sub> injection, the unconstructed Cu surface has two monoatomic surface steps (marked by triangles and outlined by black curves) on the right side of the image. (b-c) When O<sub>2</sub> is gradually injected into the specimen chamber, MRR (colored red) are first observed on upper terrace surface steps, facilitating respective growth and retreat of steps 1 and 2. (d) Following MRR formation on upper terrace surface steps, MRR is observed near lower terrace surface steps (marked by red arrow). (e) MRR on isolated flat terraces, formed by MRR phase expansion over the two terrace terminations developed by surface steps. Time scales are normalized relative to O<sub>2</sub> injection. Insets in (a-d) illustrate corresponding atomic structures of the imaged areas.

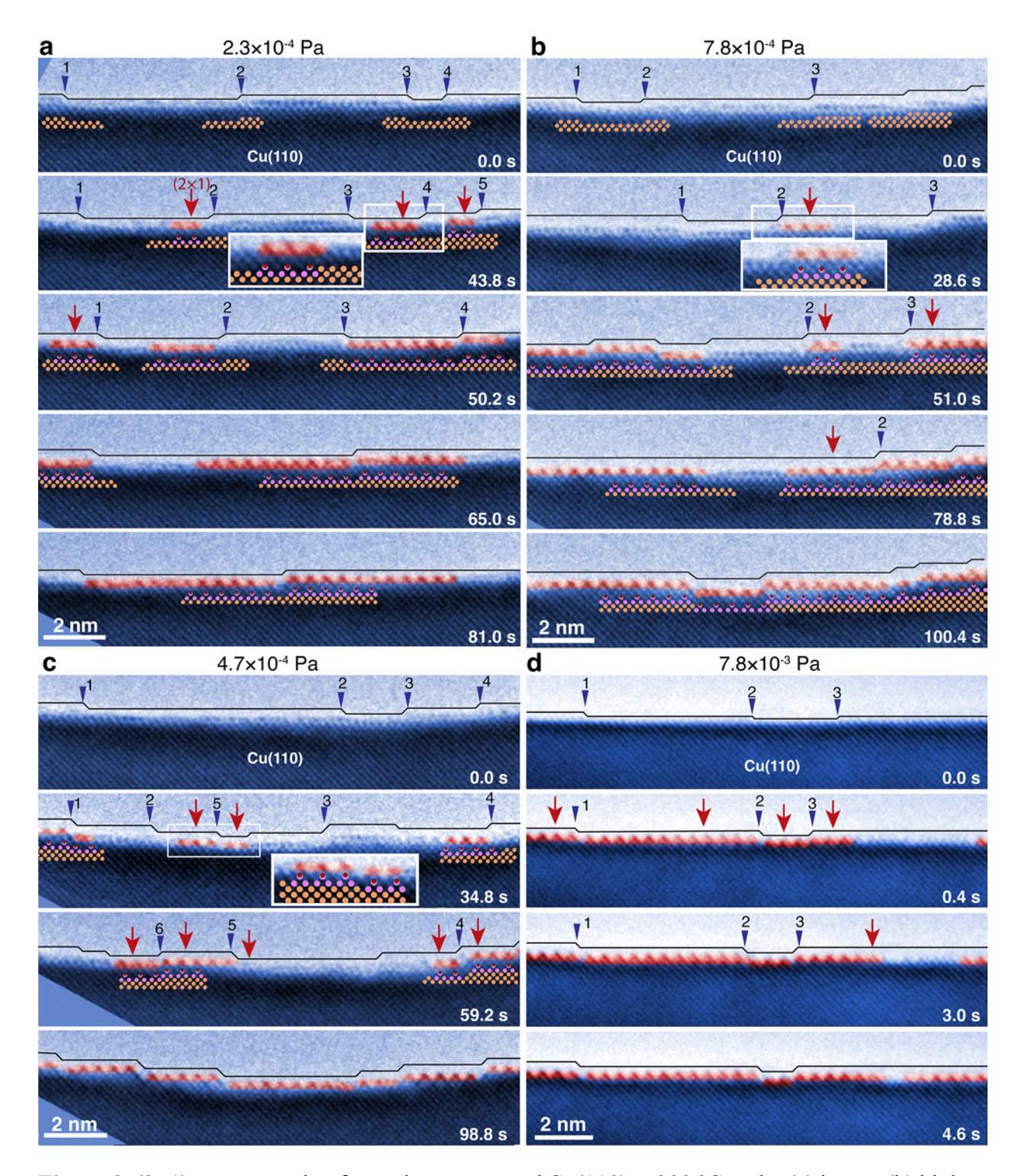


**Figure 3.** (2×1) reconstruction formation on stepped Cu(110) at 300 °C under (a) lower, (b) higher, (c) medium, and (d) very high  $O_2$  concentrations. (a) Under a lower  $O_2$  concentration of  $2.3 \times 10^{-4}$  Pa, the (2×1) reconstruction phase (colored red and marked by red arrows) is observed on the lower

terraces of steps 2, 4, and 5 first (marked by triangles and outlined by black curves), and then on the upper terraces of steps 1 and 4. (b) Under a higher  $O_2$  pressure of  $7.8 \times 10^{-4}$  Pa,  $(2\times 1)$  reconstruction forms on the upper terraces of steps 2 and 3 first, and then on the lower terrace of step 2. (c) Under a medium  $O_2$  pressure of  $4.7 \times 10^{-4}$  Pa,  $(2\times 1)$  reconstructions form on both upper and lower terraces of steps 1, 4, 5 and 6, then expands to the entire surface. (d) Under a very high  $O_2$  partial pressure of  $7.8 \times 10^{-3}$  Pa,  $(2\times 1)$  reconstructions cover the Cu(110) surface within seconds, preferring step regions over flat surfaces. Insets shows enlarged views of the boxed areas with corresponding atomic structures.

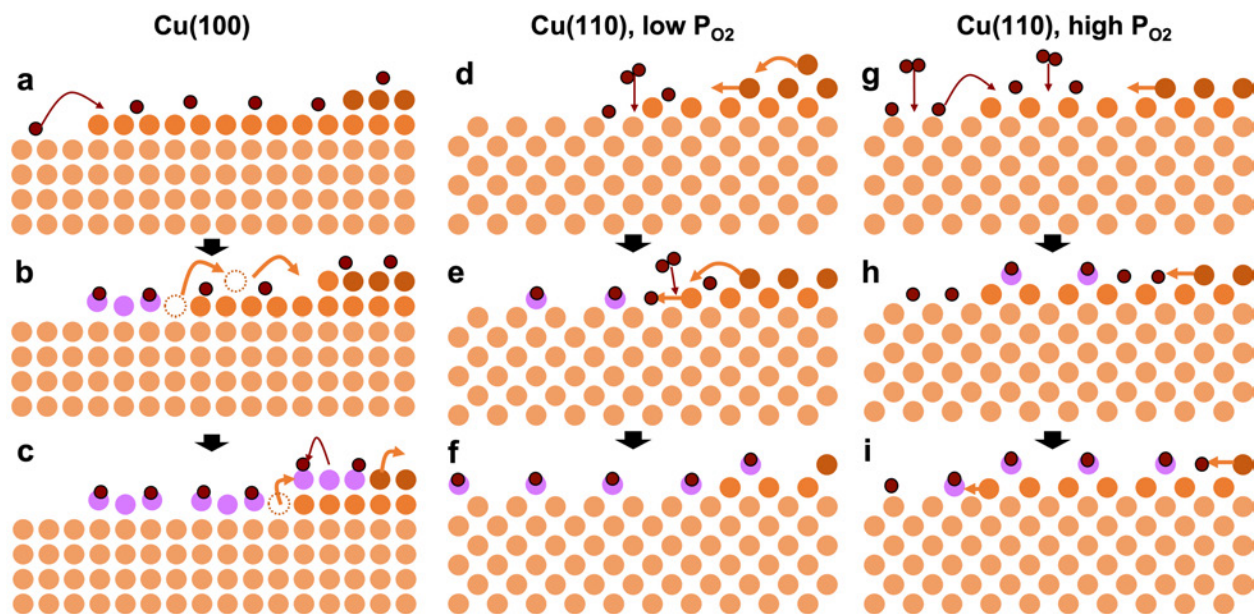


**Figure 4.** Schematic illustration showing how surface steps affect surface reconstruction on Cu(100) and Cu(110) surfaces. **(a-c)** MRR reconstruction formation on stepped Cu(100) surface. Due to the negative O diffusion E-S barrier, step ascending O diffusion is preferred. This leads to more O, and preferential MRR formation, on the upper terrace. During MRR formation, Cu surface atoms are ejected, forming missing rows via ejected Cu diffusion. Diffusing Cu can form new Cu-O chains along the step. **(d-f)** (2×1) reconstruction formation on stepped Cu(110) under low O<sub>2</sub> concentration. Under low O<sub>2</sub> concentration, the diffusing O are scare, thus O<sub>2</sub> dissociation and

absorption serve as O sources for the reconstructions. Diffusing Cu detached from step edges combine with surface adsorbed O to form "added row" Cu-O chains. O<sub>2</sub> absorbed and dissociated mainly near step edges due to preferable absorption energetics. Due to the positive Cu diffusion E-S barrier on these surface steps, descending Cu diffusion is preferred. This leads to slightly more Cu on lower terraces, resulting in preferential (2×1) phase formation on lower terraces. (g-i) (2×1) reconstruction formation on stepped Cu(110) under high O<sub>2</sub> concentration. Diffusing O reacts with diffusing Cu to form the "added row" Cu-O chains. Due to slightly preferred O accumulation on upper terraces, Cu-O chain formation on the upper terrace of the step is slightly preferred. Cu atoms (orange) from the top two layers forming the step are colored in darker shades, while the reconstructed areas are colored in magenta. O atoms are colored red.

# ASSOCIATED CONTENT

# **Supporting Information.**

Movie S1: Formation of MRR on stepped Cu(100) surface under 7×10<sup>-3</sup> Pa O<sub>2</sub> at 300 °C. (MP4)

Movie S2: Formation of MRR on stepped Cu(100) surface under 7×10<sup>-3</sup> Pa O<sub>2</sub> at 400 °C. (MP4)

Movie S3: Formation of  $(2\times1)$  reconstruction on stepped Cu(110) surface under low O<sub>2</sub> concentration  $(2.3\times10^{-4} \text{ Pa}, 300 \text{ °C})$ . (MP4)

Movie S4: Formation of  $(2\times1)$  reconstruction on stepped Cu(110) surface under high O<sub>2</sub> concentration  $(7.8\times10^{-4} \text{ Pa}, 300 \text{ °C})$ . (MP4)

Movie S5: Formation of  $(2\times1)$  reconstruction on stepped Cu(110) surface under medium O<sub>2</sub> concentration  $(4.7\times10^{-4} \text{ Pa}, 300 \text{ °C})$ . (MP4)

Movie S6: Formation of (2×1) reconstruction on stepped Cu(110) surface under higher O<sub>2</sub>

pressure  $(1.0 \times 10^{-2} \text{ Pa}, 300 ^{\circ}\text{C})$ . (MP4)

**AUTHOR INFORMATION** 

**Corresponding Authors** 

\*Correspondence to: alsaidi@pitt.edu, judyyang@pitt.edu

**Present Addresses** 

† Department of Chemical Engineering, Pohang University of Science and Technology

(POSTECH), Pohang, Gyeongbuk 37673, Republic of Korea.

**Author Contributions** 

J.C.Y. and W.A.S. conceived and directed the project. M.L. conducted the experiments, data analysis, and drafted the

manuscript. M.T.C. conducted analysis involving simulations. All authors contributed to results discussion and manuscript

refinement.

**Funding Sources** 

This work is supported by the National Science Foundation under grants DMR-1410055 (M.T.C., W.A.S, J.C.Y.), DMR-

1508417 (M.L., W.A.S., J.C.Y.), and CMMI-1905647 (M.L, W.A.S.).

ACKNOWLEDGMENT

19

We acknowledge Dr. Xianhu Sun (SUNY Binghamton), Mr. Richard Burke Garza, and Dr. Stephen D. House (University of Pittsburgh) for helpful discussions and assistance in experiments and theory. The experimental work was performed at the Petersen Institute of NanoScience and Engineering (PINSE) Nanoscale Fabrication and Characterization Facility (NFCF) at the University of Pittsburgh. We thank NFCF staff Mr. Matt France and Dr. Susheng Tan for their assistance. This research used resources of the Environmental TEM Catalysis Consortium (ECC), which is supported by the University of Pittsburgh and Hitachi High Technologies. Computational resources were provided by the University of Pittsburgh Center for Research Computing (CRC), and the Extreme Science and Engineering Discovery Environment (XSEDE) supported by the National Science Foundation (NSF OCI-1053575). This work is supported by the National Science Foundation under grants DMR-1410055 (M.T.C, W.A.S, J.C.Y), DMR-1508417(M.L, W.A.S, J.C.Y), and CMMI-1905647(M.L, W.A.S).

#### REFERENCES

- 1. Zambelli, T.; Wintterlin, J.; Trost, J.; Ertl, G. Identification of the "Active Sites" of a Surface-Catalyzed Reaction. *Science* **1996**, 273, (5282), 1688-1690.
- 2. Hagman, B.; Posada-Borbon, A.; Schaefer, A.; Shipilin, M.; Zhang, C.; Merte, L. R.; Hellman, A.; Lundgren, E.; Gronbeck, H.; Gustafson, J. Steps Control the Dissociation of CO2 on Cu(100). *J Am Chem Soc* **2018**, 140, (40), 12974-12979.
- 3. Fester, J.; García-Melchor, M.; Walton, A. S.; Bajdich, M.; Li, Z.; Lammich, L.; Vojvodic, A.; Lauritsen, J. V. Edge reactivity and water-assisted dissociation on cobalt oxide nanoislands. *Nature Communications* **2017**, **8**, 6-13.
- 4. Tao, F.; Dag, S.; Wang, L. W.; Liu, Z.; Butcher, D. R.; Bluhm, H.; Salmeron, M.; Somorjai, G. A. Break-up of stepped platinum catalyst surfaces by high CO coverage. *Science* **2010**, 327, (5967), 850-3.
- 5. Vang, R. T.; Honkala, K.; Dahl, S.; Vestergaard, E. K.; Schnadt, J.; Laegsgaard, E.; Clausen, B. S.; Norskov, J. K.; Besenbacher, F. Controlling the catalytic bond-breaking selectivity of Ni surfaces by step blocking. *Nat Mater* **2005**, **4**, (2), 160-2.
- 6. Dvorak, F.; Farnesi Camellone, M.; Tovt, A.; Tran, N. D.; Negreiros, F. R.; Vorokhta, M.; Skala, T.; Matolinova, I.; Myslivecek, J.; Matolin, V.; Fabris, S. Creating single-atom Pt-ceria catalysts by surface step decoration. *Nat Commun* **2016**, *7*, 10801.

- 7. Maiti, K.; Maiti, S.; Curnan, M. T.; Kim, H. J.; Han, J. W. Engineering Single Atom Catalysts to Tune Properties for Electrochemical Reduction and Evolution Reactions. *Advanced Energy Materials* **2021**, 11, (38).
- 8. Hendriksen, B. L.; Ackermann, M. D.; van Rijn, R.; Stoltz, D.; Popa, I.; Balmes, O.; Resta, A.; Wermeille, D.; Felici, R.; Ferrer, S.; Frenken, J. W. The role of steps in surface catalysis and reaction oscillations. *Nat Chem* **2010**, *2*, (9), 730-4.
- 9. Cabrera, N.; Burton, W. K. Crystal growth and surface structure. Part II. *Discussions of the Faraday Society* **1949**, 5, 40-48.
- 10. Schwoebel, R. L.; Shipsey, E. J. Step Motion on Crystal Surfaces. *Journal of Applied Physics* **1966**, 37, (10), 3682-3686.
- 11. Gattinoni, C.; Michaelides, A. Atomistic details of oxide surfaces and surface oxidation: the example of copper and its oxides. *Surface Science Reports* **2015**, 70, (3), 424-447.
- 12. Zhu, Q.; Zou, L.; Zhou, G.; Saidi, W. A.; Yang, J. C. Early and transient stages of Cu oxidation: Atomistic insights from theoretical simulations and in situ experiments. *Surface Science* **2016**, 652, 98-113.
- 13. Hansen, P. L. Atom-Resolved Imaging of Dynamic Shape Changes in Supported Copper Nanocrystals. *Science* **2002**, 295, (5562), 2053-2055.
- 14. Luc, W.; Fu, X.; Shi, J.; Lv, J.-J.; Jouny, M.; Ko, B. H.; Xu, Y.; Tu, Q.; Hu, X.; Wu, J.; Yue, Q.; Liu, Y.; Jiao, F.; Kang, Y. Two-dimensional copper nanosheets for electrochemical reduction of carbon monoxide to acetate. *Nature Catalysis* **2019**, *2*, (5), 423-430.
- 15. McKee, R. A.; Walker, F. J.; Chisholm, M. F. Physical structure and inversion charge at a semiconductor interface with a crystalline oxide. *Science* **2001**, 293, (5529), 468-471.
- 16. Cong, S.; Tian, Y.; Li, Q.; Zhao, Z.; Geng, F. Single-crystalline tungsten oxide quantum dots for fast pseudocapacitor and electrochromic applications. *Advanced Materials* **2014**, 26, (25), 4260-4267.
- 17. Zhu, Q.; Saidi, W. A.; Yang, J. C. Enhanced Mass Transfer in the Step Edge Induced Oxidation on Cu(100) Surface. *The Journal of Physical Chemistry C* **2017**, 121, (21), 11251-11260.
- 18. Zhu, Q.; Saidi, W. A.; Yang, J. C. Step-Edge Directed Metal Oxidation. *J Phys Chem Lett* **2016**, 7, (13), 2530-6.
- 19. Zhu, Q.; Saidi, W. A.; Yang, J. C. Step-Induced Oxygen Upward Diffusion on Stepped Cu(100) Surface. *The Journal of Physical Chemistry C* **2014**, 119, (1), 251-261.
- 20. Curnan, M. T.; Andolina, C. M.; Li, M.; Zhu, Q.; Chi, H.; Saidi, W. A.; Yang, J. C. Connecting Oxide Nucleation and Growth to Oxygen Diffusion Energetics on Stepped Cu(011) Surfaces: An Experimental and Theoretical Study. *The Journal of Physical Chemistry C* **2018**, 123, (1), 452-463.
- 21. Okada, M.; Vattuone, L.; Gerbi, A.; Savio, L.; Rocca, M.; Moritani, K.; Teraoka, Y.; Kasai, T. Unravelling the Role of Steps in Cu2O Formation via Hyperthermal O2 Adsorption at Cu(410). *The Journal of Physical Chemistry C* **2007**, 111, (46), 17340-17345.
- 22. Zhou, G.; Luo, L.; Li, L.; Ciston, J.; Stach, E. A.; Yang, J. C. Step-edge-induced oxide growth during the oxidation of Cu surfaces. *Physical Review Letters* **2012**, 109, (23), 1-5.
- 23. Lampimaki, M.; Lahtonen, K.; Hirsimaki, M.; Valden, M. Nanoscale oxidation of Cu100: oxide morphology and surface reactivity. *J Chem Phys* **2007**, 126, (3), 034703.
- 24. Yang, J. C.; Yeadon, M.; Kolasa, B.; Gibson, J. M. Surface Reconstruction and Oxide Nucleation Due to Oxygen Interaction with Cu(001) Observed by In Situ Ultra-High Vacuum Transmission Electron Microscopy. *Microsc Microanal* **1998**, 4, (3), 334-339.

- 25. Yuan, W.; Wang, Y.; Li, H.; Wu, H.; Zhang, Z.; Selloni, A.; Sun, C. Real-Time Observation of Reconstruction Dynamics on TiO2(001) Surface under Oxygen via an Environmental Transmission Electron Microscope. *Nano Lett* **2016**, 16, (1), 132-7.
- 26. Li, M.; Curnan, M. T.; Gresh-Sill, M. A.; House, S. D.; Saidi, W. A.; Yang, J. C. Unusual layer-by-layer growth of epitaxial oxide islands during Cu oxidation. *Nat Commun* **2021**, 12, (1), 2781.
- 27. Chi, H.; Curnan, M. T.; Li, M.; Andolina, C. M.; Saidi, W. A.; Veser, G.; Yang, J. C. In situ environmental TEM observation of two-stage shrinking of Cu2O islands on Cu(100) during methanol reduction. *Phys Chem Chem Phys* **2020**, 22, (5), 2738-2742.
- 28. Li, M.; Xie, D. G.; Zhang, X. X.; Yang, J. C.; Shan, Z. W. Quantifying Real-Time Sample Temperature Under the Gas Environment in the Transmission Electron Microscope Using a Novel MEMS Heater. *Microsc Microanal* **2021**, 27, (4), 758-766.
- 29. Song, M.; Zhou, G.; Lu, N.; Lee, J.; Nakouzi, E.; Wang, H.; Li, D. Oriented attachment induces fivefold twins by forming and decomposing high-energy grain boundaries. *Science* **2020**, 367, (6473), 40-45.
- 30. Jensen, F.; Besenbacher, F.; Laegsgaard, E.; Stensgaard, I. I. Dynamics of oxygen-induced reconstruction of Cu(100) studied by scanning tunneling microscopy. *Phys Rev B Condens Matter* **1990**, 42, (14), 9206-9209.
- 31. Kittel, M.; Polcik, M.; Terborg, R.; Hoeft, J. T.; Baumgärtel, P.; Bradshaw, A. M.; Toomes, R. L.; Kang, J. H.; Woodruff, D. P.; Pascal, M.; Lamont, C. L. A.; Rotenberg, E. The structure of oxygen on Cu(100) at low and high coverages. *Surface Science* **2001**, 470, (3), 311-324.
- 32. Duan, X.; Warschkow, O.; Soon, A.; Delley, B.; Stampfl, C. Density functional study of oxygen on Cu(100) and Cu(110) surfaces. *Physical Review B* **2010**, 81, (7), 1-15.
- 33. Saidi, W. A.; Lee, M.; Li, L.; Zhou, G.; McGaughey, A. J. H. Ab initioatomistic thermodynamics study of the early stages of Cu(100) oxidation. *Physical Review B* **2012**, 86, (24), 1-8.
- 34. Jensen, F.; Besenbacher, F.; Laegsgaard, E.; Stensgaard, I. I. Surface reconstruction of Cu(110) induced by oxygen chemisorption. *Phys Rev B Condens Matter* **1990**, 41, (14), 10233-10236.
- 35. Leibsle, F. M. STM studies of oxygen-induced structures and nitrogen coadsorption on the Cu(100) surface: evidence for a one-dimensional oxygen reconstruction and reconstructive interactions. *Surface Science* **1995**, 337, (1-2), 51-66.
- 36. Liu, Q.; Li, L.; Cai, N.; Saidi, W. A.; Zhou, G. Oxygen chemisorption-induced surface phase transitions on Cu(110). *Surface Science* **2014**, 627, 75-84.
- 37. Balkenende, A. R.; Hoogendam, R.; de Beer, T.; Gijzeman, O. L. J.; Geus, J. W. The interaction of NO, O2 and CO with Cu(710) and Cu(711). *Applied Surface Science* **1992**, 55, (1), 1-9.
- 38. Ge, J.-Y.; Dai, J.; Zhang, J. Z. H. Dissociative Adsorption of O2 on Cu(110) and Cu(100): Three-Dimensional Quantum Dynamics Studies. *The Journal of Physical Chemistry* **1996**, 100, (27), 11432-11437.
- 39. Li, L.; Cai, N.; Saidi, W. A.; Zhou, G. Role of oxygen in Cu(1 1 0) surface restructuring in the vicinity of step edges. *Chemical Physics Letters* **2014**, 613, 64-69.
- 40. Coulman, D. J.; Wintterlin, J.; Behm, R. J.; Ertl, G. Novel mechanism for the formation of chemisorption phases: The (2×1)O-Cu(110) added row reconstruction. *Physical Review Letters* **1990**, 64, (15), 1761-1764.

- 41. Lian, X.; Xiao, P.; Liu, R.; Henkelman, G. Calculations of Oxygen Adsorption-Induced Surface Reconstruction and Oxide Formation on Cu(100). *Chemistry of Materials* **2017**, 29, (4), 1472-1484.
- 42. Lian, X.; Xiao, P.; Liu, R.; Henkelman, G. Communication: Calculations of the (2 x 1)-O reconstruction kinetics on Cu(110). *J Chem Phys* **2017**, 146, (11), 111101.
- 43. Rabbering, F.; Wormeester, H.; Everts, F.; Poelsema, B. Quantitative understanding of the growth of Cu/Cu(001) including the determination of the Ehrlich-Schwoebel barrier at straight steps and kinks. *Physical Review B* **2009**, 79, (7), 1-10.
- 44. Liem, S. Y.; Clarke, J. H. R.; Kresse, G. Pathways to dissociation of O2 on Cu (110) surface: first principles simulations. *Surface Science* **2000**, 459, (1-2), 104-114.